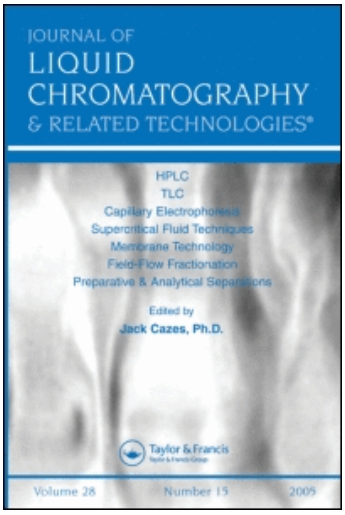


**Journal of Liquid Chromatography & Related Technologies**
Publication details, including instructions for authors and subscription information:
http://www.informaworld.com/smpp/title~content=t713597273

# Effect of Subdividing the Adsorbent Bed in a Five-Zone Simulated Moving Bed Chromatography for Ternary Separation

Sungyong Mun[a]
[a] Department of Chemical Engineering, Hanyang University, Seoul, Korea

**To cite this Article** Mun, Sungyong(2008) 'Effect of Subdividing the Adsorbent Bed in a Five-Zone Simulated Moving Bed Chromatography for Ternary Separation', Journal of Liquid Chromatography & Related Technologies, 31: 9, 1231 — 1257
**To link to this Article: DOI:** 10.1080/10826070802022354
**URL:** http://dx.doi.org/10.1080/10826070802022354

*Journal of Liquid Chromatography & Related Technologies*®, 31: 1231–1257, 2008

ISSN 1082-6076 print/1520-572X online
DOI: 10.1080/10826070802022354

# Effect of Subdividing the Adsorbent Bed in a Five-Zone Simulated Moving Bed Chromatography for Ternary Separation

**Sungyong Mun**

Department of Chemical Engineering, Hanyang University, Seoul, Korea



**Abstract:** A five-zone simulated moving bed (SMB) chromatography, which has been successful in achieving a ternary separation so far, was optimized in this study to separate three nucleoside components (2′-deoxycytidine, 2′-deoxyguanosine, and 2′-deoxyadenosine) with high purity. For such an optimized process, we investigated how the subdivision of its chromatographic bed affects the wave dynamics and separation performance, which has been one of the important issues in the area of a continuous chromatographic separation process design. It was found that the migration or propagation behavior of the highest affinity component (2′-deoxyadenosine) virtually controlled the wave dynamics and separation performance of the five-zone SMB chromatography. Unlike the lowest affinity and the intermediate affinity components (2′-deoxycytidine and 2′-deoxyguanosine), the highest affinity component generated more than two solute bands, which were scattered in several zones. As the degree of bed subdivision became higher, the scattered solute bands of the highest affinity component were gradually merged, leading to a seemingly single solute band with a wavy plateau. Eventually, the wavy plateau became flat. Such behavior of the highest affinity component brought about a visible change in its average concentrations at the two product ports, and a significant reduction in the purity of the intermediate affinity component. The results of this study can serve as a useful summary of five-zone SMB behaviors, and as the first step for the development of new strategies on five-zone SMB performance.

**Keywords:** Five-zone SMB, Bed subdivision, Wave dynamics, Separation performance

Correspondence: Prof. Sungyong Mun, Department of Chemical Engineering, Hanyang University, Haengdand-dong, Seongdong-gu, Seoul 133-791, Korea. E-mail: munsy@hanyang.ac.kr

## INTRODUCTION

In chromatographic separation processes, a mode of countercurrent contact between the liquid and solid (or adsorbent) phases is usually more advantageous in terms of adsorbent utilization and solvent usage than a batch operation mode.[1,2] Such an advantage is mostly attributed to the fact that the mass transfer driving force becomes maximized in a countercurrent contact system, in which the solid phase is moving in the direction opposite to the liquid phase.[1] The application of such a countercurrent contact mode to chromatographic separation processes has been chiefly exemplified by a true moving bed (TMB) in the literature.[1,3,4] The TMB operation, however, leads to particle attrition and imposes severe limitations on the mechanical properties of the adsorbent particles due to the physical movement of solids. To avoid such problems, a TMB has been replaced by a simulated moving bed (SMB), where the effect of countercurrent contact is simulated by moving the inlet and outlet ports at a fixed time interval in the direction of desorbent flow.[1,3,4]

Since a perfect countercurrent contact effect is indeed unattainable in SMB, some discrepancies in the behavior of a concentration wave propagation and migration through the adsorbent bed (or wave dynamics) are inevitable between SMB and TMB. The discrepancies in the wave dynamics may also bring about a difference in the separation performance between the two chromatographic processes.

In the case of a classical four-zone or a three-zone process for binary separation (Figure 1), the wave dynamics and separation performance of SMB were found to be different from those of its corresponding TMB.[1,3,4] It was also reported that such differences between a four-zone SMB and its corresponding TMB become smaller as each of the four zones in SMB is divided into a larger number of subdivisions.[1,3,4] By contrast, the difference in the wave dynamics between a three-zone SMB and its corresponding TMB was reported to remain virtually unchanged regardless of an increase in the number of subdivisions in each zone.[1] These phenomena indicate that subdividing the adsorbent bed can have a different effect on the wave dynamics and separation performance of an SMB system depending on its structure or configuration, which has been worthy of research in the area of a continuous chromatographic separation process.

As stated above, the effect of the bed subdivisions has been extensively studied with regard to a classical four-zone or a three-zone SMB for binary separation (Figure 1). Such issues, however, have been rarely handled with regard to a single cascade SMB containing more than four zones for the purpose of multi-component separation. One of the recently developed SMBs for such a purpose is a five-zone SMB process (Figure 2a), which aims to separate a ternary mixture into three different pure fractions using only a single unit.[5–7] Most of the previous studies regarding a five-zone SMB for ternary separation[5–7] have been focused on the design, optimization, and modeling. No previous studies have, hitherto, given a detailed explanation of

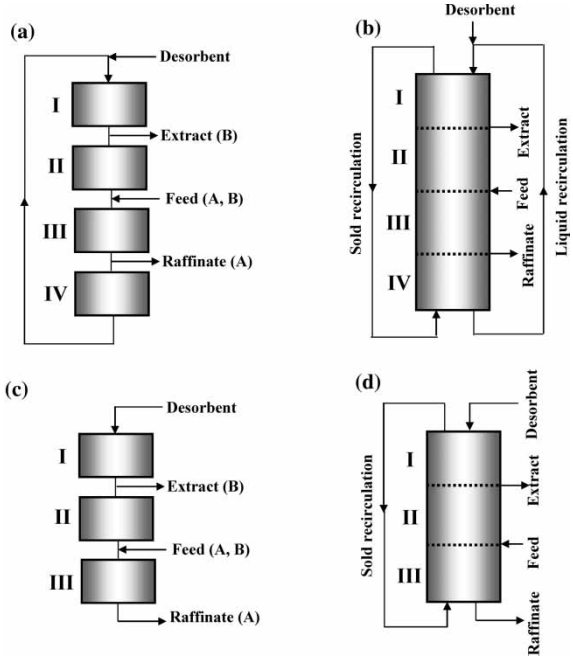


***Figure 1.*** (a) Classical four-zone SMB for binary separation (Switching of ports is not shown.). (b) Classical four-zone TMB for binary separation. (c) Three-zone SMB for binary separation (Switching of ports is not shown.). (d) Three-zone TMB for binary separation. A: low-affinity solute, B: high-affinity solute.



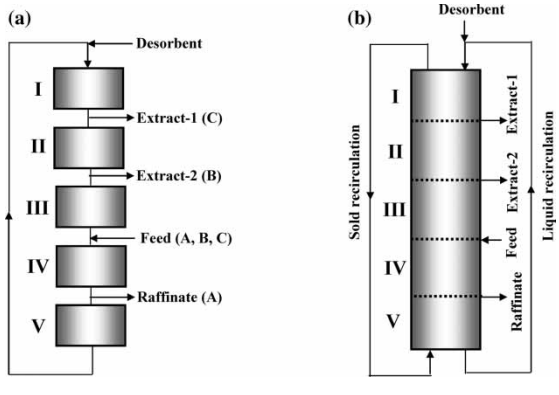


***Figure 2.*** (a) Five-zone SMB for ternary separation (Switching of ports is not shown.). (b) Five-zone TMB for ternary separation. A: lowest-affinity solute, B: intermediate-affinity solute, C: highest-affinity solute.

how the bed subdivision influences the wave dynamics and separation performance of a five-zone SMB for ternary separation.

The goal of this study is to investigate the effect of subdividing the adsorbent bed on the wave dynamics in a five-zone SMB for ternary separation. The separation performance of a five-zone SMB will also be examined by increasing the number of subdivisions in each zone. The resulting change in the separation performance from the bed subdivision will be again discussed from the standpoint of wave dynamics. Finally, the wave dynamics and separation performance of a five-zone SMB will be compared with those of its corresponding five-zone TMB, which is virtually equivalent to a five-zone SMB with an infinite number of subdivisions in each zone.

For this purpose, the system of a ternary nucleoside mixture (2′-deoxycytidine, 2′-deoxyguanosine, 2′-deoxyadenosine)[8,9] is chosen as a model system. The adsorbent used for the separation of the model system is SOURCE 30RPC, where 2′-deoxycytidine has the lowest affinity, 2′-deoxyguanosine the intermediate affinity, and 2′-deoxyadenosine the highest affinity.[8,9] We first determined the optimal operating conditions of a five-zone SMB with one column per zone using an adaptation of the state of the art optimization method, non dominated sorting genetic algorithm with elitism and jumping genes (NSGA-II-JG).[10–13] For the five-zone SMB optimized as above, the dynamic wave propagation phenomena during a transient period are examined together with the dynamic wave migration phenomena at a cyclic steady state. Then, the adsorbent bed of each zone is divided into an increasing number of subdivisions while keeping the total bed volume unchanged. Such effect on the wave dynamics and separation performance are investigated by using a series of column profiles and effluent histories, which are obtained from detailed simulations.



## PRINCIPLE OF TERNARY SEPARATION IN A FIVE-ZONE SMB

For the sake of convenience, three mixture components to be separated are denoted as A, B, and C, where component A has the lowest adsorption affinity and component C the highest adsorption affinity. Component B thus corresponds to an intermediate affinity component in a ternary mixture. Among the three nucleosides chosen as a model system in this study, 2′-deoxycytidine corresponds to component A, while 2′-deoxyguanosine and 2′-deoxyadenosine correspond to components B and C, respectively. To separate such a ternary mixture into three different pure fractions in a single unit, one can use a five-zone SMB, whose structure is depicted in Figure 2a.

Note that three product ports are located in a five-zone SMB (Figure 2a). Among them, the product ports for the lowest-affinity (A) and the highest-affinity (C) components are located on the other side of the feed port as in a classical four-zone SMB. An additional product port, which is used to

obtain the intermediate affinity component (B), is located upstream from the feed port, such that the five-zone SMB has two extract ports.[5–7]

If the operating conditions of the five-zone SMB are properly designed, component A will migrate downstream from the feed port and reach the raffinate port. At the same time, components B and C will migrate upstream from the feed port and exit from the extract 2 and the extract 1 ports, respectively. Such migration trends can guarantee only the separation of A from B and C. Additional separation load, which is to separate B from C, imposes the following restrictions on component C; most of the component C molecules injected into the feed port should be confined within one column until they enter zone I by a series of port switchings. This is to prevent the passage of component C through the extract 2 port, thereby obtaining a high purity of B in the extract 2 stream and high recovery of C in the extract 1 stream. Because of such restriction on the component C migration behavior, the feasibility of the aforementioned five-zone SMB is usually subject to the selectivity between B and C.[5–7]



## MATHEMATICAL MODEL

The mathematical model is based on differential mass balance equations for both the mobile phase and the stationary phase. The model equations consider convection, axial dispersion, and film mass transfer. The details of the model equations can be found elsewhere.[8]

The feed concentrations of the three nucleoside components ($C_{F,A} = 1.0$ g/L, $C_{F,B} = 1.0$ g/L, $C_{F,C} = 1.0$ g/L), which are kept the same as those in the previous study,[8] are in the region of a linear isotherm relation. The linear isotherm constants and the other intrinsic parameters were reported by Hur et al.,[8] and they are summarized in Table 1.

To solve the aforementioned model equations, a biased upwind differencing scheme (BUDS) was employed in conjunction with the Implicit Euler integration method. All of these numerical computations are carried out in Aspen Chromatography 2004.1. simulator, which has been validated in several previous studies.[6,8,15–17]

## RESULTS AND DISCUSSION

### Optimization of a Five-Zone SMB Chromatography for the Separation of a Ternary Nucleoside Mixture

Column profiles and effluent histories can be effectively used to investigate the effect of subdividing the adsorbent bed on the wave dynamics and separation performance of a five-zone SMB. To obtain the column profiles and effluent histories, the operating conditions such as zone flow rates and step time

***Table 1.*** Isotherm constants and intrinsic parameters of the three nucleoside components[a]

| | 2′-deoxycytidine (A) | 2′-deoxyguanosine (B) | 2′-deoxyadenosine (C) |
|---|---|---|---|
| Linear isotherm constant at T = 30°C | 3.15 | 7.40 | 27.7 |
| Mass transfer coefficient, (1/s) | 1.0 | 0.5 | 0.1 |
| Axial dispersion coefficient ($cm^2$/min) | The Chung and Wen correlation[14] | | |
| Total void fraction | 0.80 | | |
| Particle diameter (μm) | 30.0 | | |
| Fluid density (g/$cm^3$) | 1.0 | | |
| Viscosity (cP) | 1.0 | | |
| Feed concentration (g/L) | 1.0 | | |
| Adsorbent | Source 30RPC | | |
| Desorbent | Water with 4% ethanol | | |

[a]All the data in this table were taken from the reference by Hur and Wankat.[8]

need to be determined first, such that three nucleoside products can be almost completely separated. For this purpose, a five-zone SMB with the column configuration of 1 – 1 – 1 – 1 – 1 was optimized to achieve the highest purity index obtainable. The purity index[15] is defined here as the average of the purities of the three nucleosides as follows:

$$\mathrm{PI} = \frac{(\mathrm{PurA}) + (\mathrm{PurB}) + (\mathrm{Pur\ C})}{3} \tag{1}$$

where components A, B, and C are 2′-deoxycytidine, 2′-deoxyguanosine, and 2′-deoxyadenosine, respectively. While employing the purity index as an objective function, some additional constraints were taken into account as shown below:

$$\text{Max} \qquad J = \mathrm{PI}[Q_1, D, E_1, R, t_s] \tag{2a}$$

$$\text{Subject to} \qquad \mathrm{PurA} \geq 95\%, \quad \mathrm{PurB} \geq 95\%, \quad \mathrm{PurC} \geq 95\% \tag{2b}$$

$$\Delta P_{\mathrm{unit}} \leq 10\ \mathrm{bar} \tag{2c}$$

$$\text{Fixed variables} \quad N_{\mathrm{cln}} = 5, \quad L_c = 15\,\mathrm{cm}, \quad d_c = 1\,\mathrm{cm}, \quad F = 0.5\,\mathrm{mL/min} \tag{2d}$$

$$\text{Dependent variables} \quad Q_2, Q_3, Q_4, Q_5, E_2 \tag{2e}$$

where $Q_j$ is the flow rate in zone j; D and R are the desorbent and raffinate flow rates, respectively; $E_1$ and $E_2$ are the extract 1 and extract 2 flow rates, respectively; F and $t_s$ are the feed flow rate and the step time, respectively; PurA, Pur B, and Pur C are the purities of components A, B, and C, respectively; and $\Delta P_{\mathrm{unit}}$ is the pressure drop through an SMB unit.

Equation (2b) in the above expression indicates that the purities of the three nucleoside products must be over 95% each. The reason for introducing such purity constraint is that the maximization of only a purity index may not always ensure the complete separation of all the three products. Sometimes, one of the nucleosides tends to have too high purity at the expense of the other. Such an unbalanced distribution of product purities can be prevented by using the aforementioned purity constraint.

Since the adsorbent, SOURCE 30RPC, used for the separation of the nucleoside mixture has a maximum allowable pressure drop of 10 bar,[8] the pressure drop over the entire SMB unit must be kept below 10 bar. In this study, the pressure drop of a five-zone SMB unit was taken as the sum of the pressure drops occurring in each of the five zones, which was estimated using the Ergun equation.[18] Such pressure drop constraint directly places a limit on the zone flow rate during the optimization.

The purity constraints (Eq. (2b)), which indicate the lowest purity to be attained in each product stream, were incorporated using the penalty function as described by Zhang et al.[11] and Subramani et al.[12] The modified objective function in this case can be expressed as:

$$\text{Min} \qquad I = \frac{1}{1+J} + w\sum_{i=1}^{2} f_i^2 \tag{3a}$$

where

$$f_1 = [\text{PurA} - 95] - |[\text{PurA} - 95] \tag{3b}$$

$$f_2 = [\text{PurB} - 95] - |[\text{PurB} - 95] \tag{3c}$$

$$f_3 = [\text{PurC} - 95] - |\text{PurC} - 95] \tag{3d}$$

where a large weighting factor, $w$ ($=10^4$) was used to meet the purity constraint (PurA, PurB, PurC $\geq$95%) while maximizing the objective function $J$.

For the optimization of the five-zone SMB as above, an up to date genetic algorithm such as NSGA-II-JG[10–13] was applied in combination with Excel VBA (Visual Basic Application), which has the function of controlling Aspen Chromatography. The concept of the genetic algorithm (GA) is based on the imitation of the process of natural selection and natural genetics,[10] and the successful applications of the GA to SMB optimizations have been reported in several previous publications.[11–13] The GA optimization begins with the specification of several GA parameters such as population size, the length of chromosome, the number of generations, crossover probability, mutation probability, and jumping gene probability.

Table 2 lists the GA parameters used in the optimization of the five-zone SMB. Considering both accuracy and calculation time, we chose 50 chromosomes and stopped the iteration after 80 generations. In order to ensure that the global optimum was obtained, three optimization runs were performed with different sets of initial pool of chromosomes. The optimization results listed

*Table 2.* GA parameters used in the optimization of the five-zone SMB chromatography

| Parameter | Value |
|---|---|
| Population size | 50 |
| Number of generations | 80 |
| Length of chromosome | 65 bits |
| Crossover probability | 0.9 |
| Jumping gene probability | 0.7 |
| Mutation probability | 1/(length of chromosome) |

in Table 3 show that the five-zone SMB at its global optimum achieves over 95% purity for each nucleoside product.



## Wave Dynamics and Effluent Histories of the Five-Zone SMB Chromatography with One Column Per Zone

In the previous section, a five-zone SMB with one column per zone was optimized to separate a ternary nucleoside mixture into three different pure fractions. For the optimized five-zone SMB, the growth of a solute band and the behavior of its wave migration through the adsorbent bed are investigated in this section through a series of column profiles from detailed

*Table 3.* Optimization results for the five-zone SMB with one column per zone

| | |
|---|---|
| Product purity | |
| Purity index (PI) (%) | 97.02 |
| Purity of A (%) | 97.39 |
| Purity of B (%) | 95.32 |
| Purity of C (%) | 98.36 |
| Values of decision variables at optimal state | |
| Zone I flow rate (mL/min) | 12.067 |
| Desorbent flow rate (mL/min) | 11.422 |
| Extract-1 flow rate (mL/min) | 8.053 |
| Raffinate flow rate (mL/min) | 2.499 |
| Step time (min) | 7.285 |
| Values of dependent variables at optimal state | |
| Zone II flow rate (mL/min) | 4.014 |
| Zone III flow rate (mL/min) | 2.644 |
| Zone IV flow rate (mL/min) | 3.144 |
| Zone V flow rate (mL/min) | 0.645 |
| Extract-2 flow rate (min) | 1.370 |

simulations. The concentration profile of each product stream as a function of time (or effluent history) is also examined.

The solute bands of the three components such as 2′-deoxycytidine (A), 2′-deoxyguanosine (B), and 2′-deoxyadenosine (C) grow during a transient period, eventually becoming fully developed at cyclic steady state. Such a series of growing process for each solute band is presented in Figure 3. During the first step, the three nucleoside components enter zone IV and migrate downstream from the feed port, as shown in Figure 3a. After the first switching, some portions of nucleosides enter zone III while the rest remain in zone IV (Figure 3b). As the port switching continues (Figures 3c to 3h), component A (the fast moving solute) advances beyond the feed port and approaches the raffinate port whereas component B and C (the slow moving solutes) lags behind the feed port and shifts toward the extract ports.

Due to continuous feed input and internal recycles that are typical of an SMB operation, the waves of components A and B propagate and their concentrations along the bed increase gradually. The internal recycle occurring between zones II and III helps enrich the concentration of component B in zone IIII (Figures 3d to 3h). Similarly, the internal recycles between zones IV and V help enrich the concentration of component A in zone IV (Figures 3d to 3h). Such a series of processes cause major portions of components A and B to be accumulated in the zones near the feed port (zones III and IV), constituting a form of solute band each, as shown in Figure 3h.

Unlike components A and B, component C does not accumulate around the feed port, but keeps moving upstream by port switching until it reaches zone I. As a consequence, the shapes of the solute bands of component C in zones III and IV at 10.5 steps (Figure 3 h) remain almost the same as those at 1.5 steps (Figure 3b). After component C enters zone I, a portion of the component C is recovered from the extract 1 port and the rest is recycled back to zone II (Figures 3e to 3 h).

Overall, components A and B each generate only one solute band whereas component C more than two solute bands. The solute bands of components A and B keep growing until a cyclic steady state is reached, leading to higher concentrations and larger band width than the solute bands of component C that no longer grow directly after its creation.

The growth of each solute band, which proceeds during the aforementioned transient period, is continued until the solute band is fully developed. Even after each solute band is fully developed, its concentration at any position relative to the feed port still varies instantaneously (Figure 4). Such an instantaneous variation makes it impossible to obtain a constant form of solute band with respect to position and time, resulting in the nonexistence of a steady state (concretely speaking, “static steady state”). However, a series of solute band migration behaviors, if observed at every switching time, exhibit a uniform pattern. As shown in Figure 4, the solute band itself is not stationary within every switching period, but its migration pattern is repeated uniformly at each switching time. Such state, where the migration

of the solute band shows a cyclic behavior in every switching period, has been defined as "cyclic steady state" in the literature.[1,4]

The solute band migrating at cyclic steady state is always accompanied by two concentration waves such as adsorption and desorption waves. It is the

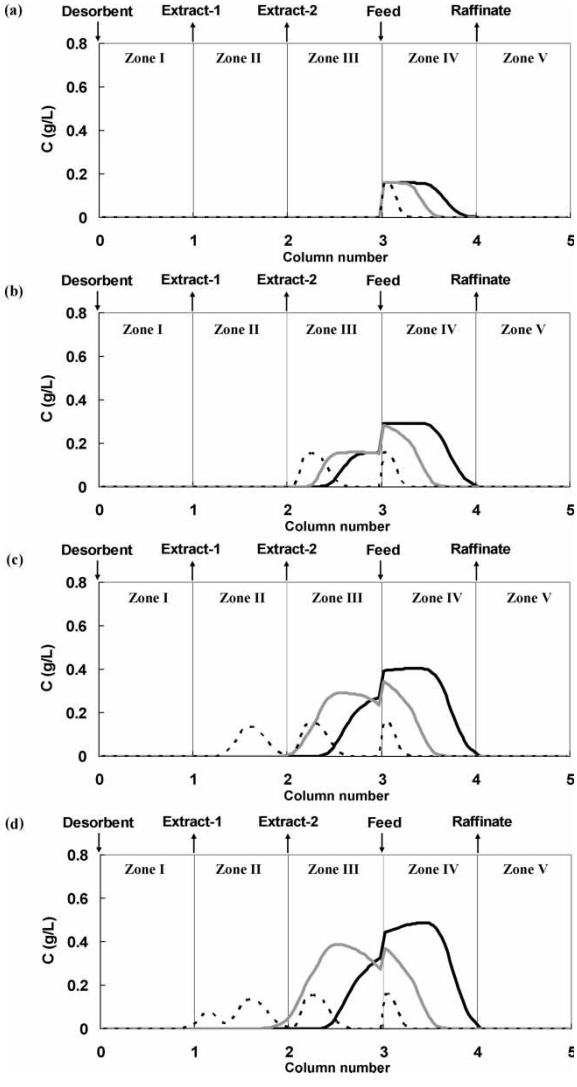


***Figure 3.*** Mid step column profiles during a transient period in the five-zone SMB with one column per zone. (a) 0.5 steps, (b) 1.5 steps, (c) 2.5 steps, (d) 3.5 steps, (e) 4.5 steps, (f) 5.5 steps, (g) 6.5 steps, (h) 10.5 steps. ▬: component A, ▬: component B, – – –: component C.

(*continued*)

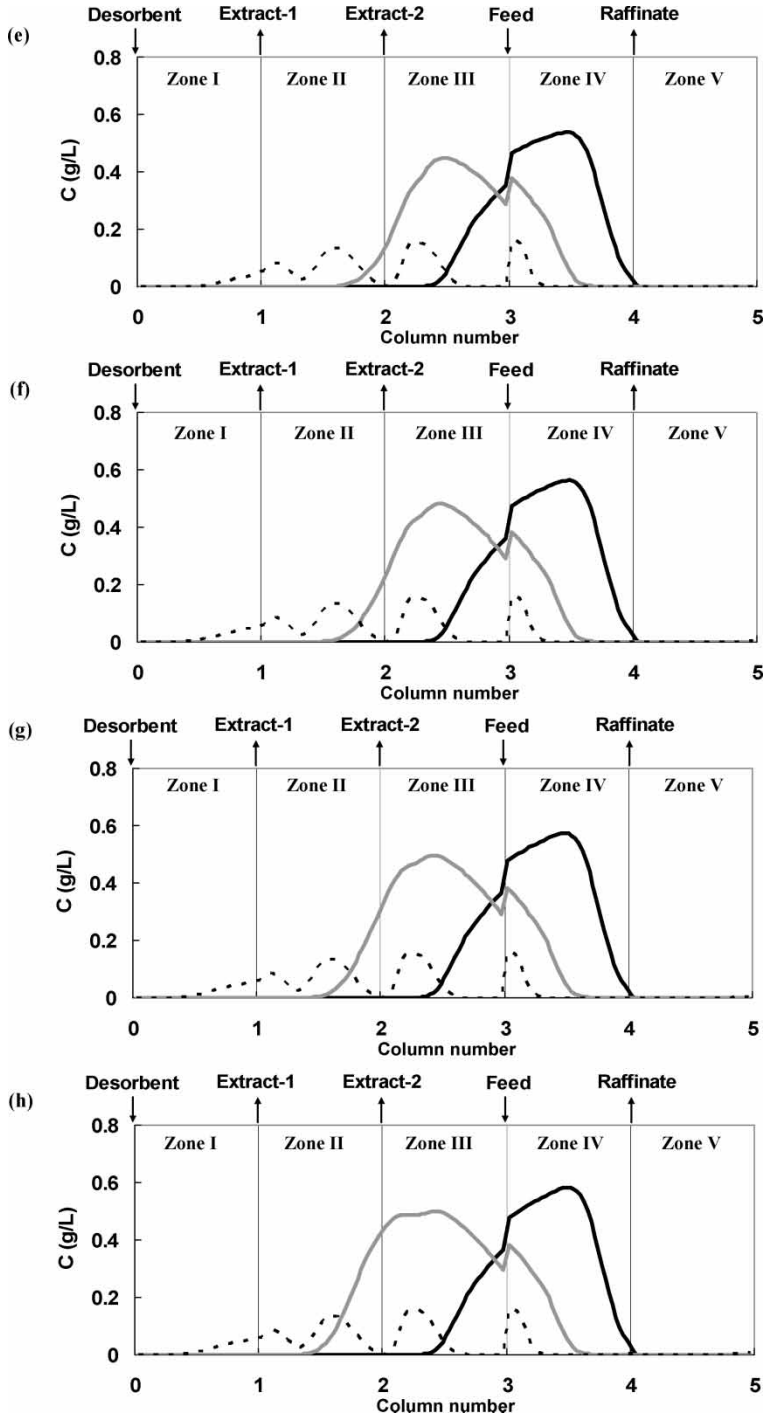


*Figure 3.* Continued.

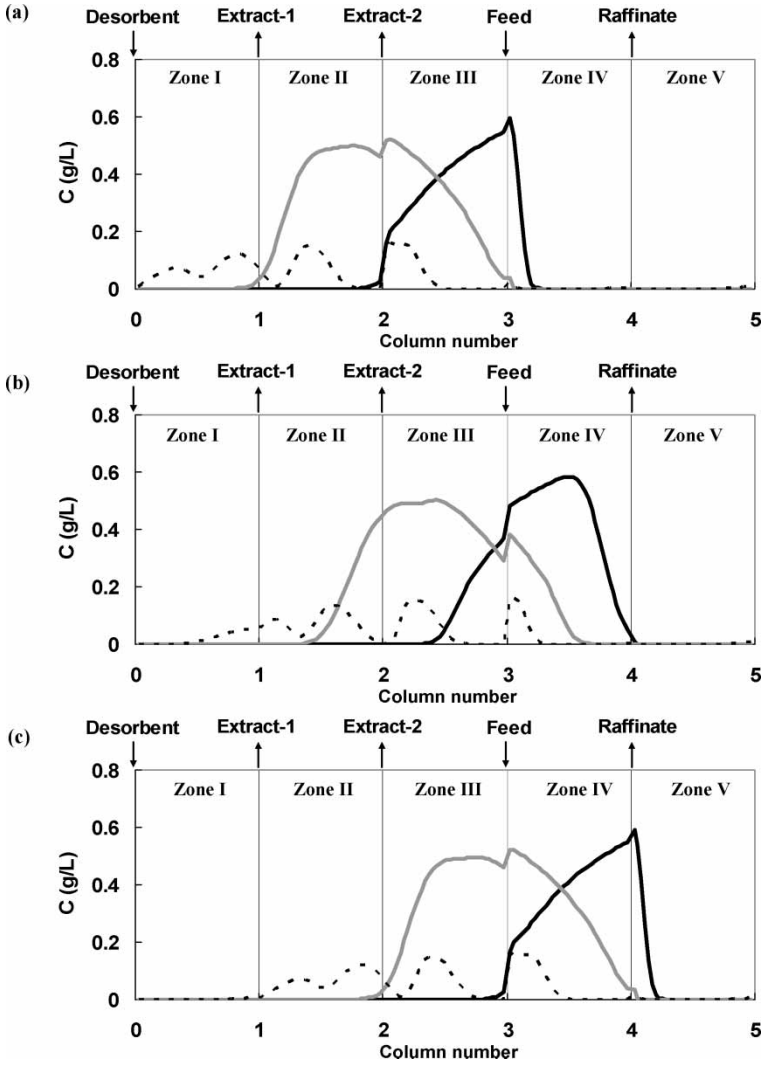


*Figure 4.* Solute band migration behaviors during the entire switching period at cyclic steady state in the five-zone SMB with one column per zone. (a) At the beginning of a step. (b) In the middle of a step. (c) At the end of a step. ▬: component A: ▬: component B,: – – – component C.

migration ranges of such two waves that virtually determine the product purities, i.e., whether complete separation occurs.[19] Note, in Figure 4, that the desorption wave of A is well confined within zones III during the entire switching period, while the adsorption wave of A is within zones IV and V. Simultaneously, the desorption and adsorption waves of B are well confined

within zones II and IV, respectively (Figure 4). Such wave conditions prevent the possible overlap of A and B at each product port, leading to almost complete separation between A and B. In addition to the A and B waves, the C wave also plays a vital role in complete ternary separation in the five-zone SMB.

As shown in Figure 4, the C wave exhibits a quite different shape and migration behavior from those of A and B waves. One interesting observation is that the adsorption wave of C is built in three different zones. The first adsorption wave of C is developed in zone IV (Figure 3a) because of its high affinity, which makes it possible for component C to be confined within the column in zone IV. Each time the port switches, the column containing the first adsorption wave of C is shifted to zone III and zone II in series. Meanwhile, the adsorption wave of C is spread due to mass transfer effects. This causes the adsorption wave of C in zone II to reach the end of the column as shown in Figure 3c. Since only a slight portion of the C wave pass through the product B stream, its effect on the purity of B is quite insignificant. Consequently, the purity of B at the extract 2 port is maintained at over 95.3%.

The effect of the C wave on the purity of A at the raffinate port is mostly governed by the migration behavior of the C desorption wave. Among the three desorption waves of C evolved, the key desorption wave of C that directly influences the purity of A is the nearest one to the desorbent port. Note, in Figure 4, that the key desorption wave of C is confined within zone I during the entire switching period, thereby preventing the possible wrap around of C from zone I to zone V. The purity of A at the raffinate port is, therefore, maintained at over 97.3%.



## Effect of Subdividing the Adsorbent Bed on the Wave Dynamics of the Five-Zone SMB Chromatography

The five-zone SMB used in the previous section was based on the absence of the bed subdivision, which means that each of the five zones contains only one column. To investigate the effect of subdividing the adsorbent bed on the wave dynamics of the five-zone SMB, the number of columns per zone is increased in this section, while the total adsorbent volume is kept the same as that of the five-zone SMB with one column per zone.

First, a series of simulations were carried out for the five-zone SMBs with an increasing number of columns per zone, while zone length and zone flow rates remained unchanged. Only the step time and single column length were reduced while the port velocity was kept constant. The operating conditions, column configuration, and column length for each SMB configuration are listed in Table 4. An extreme case occurs when an infinite number of columns will be allocated to each zone. Such an extreme case becomes equivalent to its corresponding TMB configuration.

***Table 4.*** Operating conditions and column dimensions in the five-zone SMB with an increasing number of columns per zone

| | Case I | Case II | Case III | Case IV | Case V | Case VI |
|---|---|---|---|---|---|---|
| Column configuration[a] | 1 – 1 – 1 – 1 – 1 | 2 – 2 – 2 – 2 – 2 | 4 – 4 – 4 – 4 – 4 | 6 – 6 – 6 – 6 – 6 | 8 – 8 – 8 – 8 – 8 | ∞ – ∞ – ∞ – ∞ – ∞ |
| Single column length (cm) | 15.0 | 7.5 | 3.75 | 2.5 | 1.875 | 0 |
| Column diameter (cm) | 1.0 | 1.0 | 1.0 | 1.0 | 1.0 | 1.0 |
| Zone length (cm) | 15.0 | 15.0 | 15.0 | 15.0 | 15.0 | 15.0 |
| Step time (min) | 7.285 | 3.642 | 1.821 | 1.214 | 0.9106 | 0 |
| Port velocity (cm/min) | 2.059 | 2.059 | 2.059 | 2.059 | 2.059 | 2.059 |
| Zone flow rates (mL/min) | | | | | | |
| Zone I | 12.067 | 12.067 | 12.067 | 12.067 | 12.067 | 12.067 |
| Zone II | 4.014 | 4.014 | 4.014 | 4.014 | 4.014 | 4.014 |
| Zone III | 2.644 | 2.644 | 2.644 | 2.644 | 2.644 | 2.644 |
| Zone IV | 3.144 | 3.144 | 3.144 | 3.144 | 3.144 | 3.144 |
| Zone V | 0.645 | 0.645 | 0.645 | 0.645 | 0.645 | 0.645 |

[a]Column configuration refers to the number of columns in each zone.

The column profiles for each case were obtained in the middle of a switching period at cyclic steady state, and they are shown in Figure 5. Comparison of the results from different column numbers reveals that the uneven plateaus of the solute bands of A and B become smoother as the number of columns per zone increases. The major reason for such phenomenon is that an increase in the column number per zone plays a part in dividing the plateau concentration profile more closely. This can alleviate the magnitude of any concentration variation on the plateau profile, resulting in a solute band with a smoother plateau. In the extreme case where each zone contains an infinite number of columns, the plateaus of the solute bands become completely even, which virtually correspond to the case of the five-zone TMB (Figure 5e).

Another noteworthy phenomenon is observed in the solute bands of C. They are first scattered in several zones when each zone contains only one column (Figure 5a). In the case of allocating two columns to each zone (Figure 5b), the number of the solute bands of C increases while the magnitude of each solute band of C decreases. At the same time, the scattered solute bands of C are closer to each other. When the column number per zone is further increased to four (Figure 5c), the scatted solute bands of C start to be merged, resulting in a seemingly single solute band of C with a wavy plateau. The extent of waviness in the plateau is diminished as the column number per zone is increased to eight (Figure 5d). Eventually, the wavy plateau becomes flat and the column profiles of the five-zone SMB approach those of the five-zone TMB when the column number per zone approaches infinity (Figure 5e). This phenomenon, however, has an undesirable effect on complete ternary separation, as will be explained next.



## Effect of Subdividing the Adsorbent Bed on the Effluent Histories of the Five-Zone SMB Chromatography

In addition to the wave dynamics, the effluent histories are also affected by the subdivision of the adsorbent bed. To examine such effects, the effluent histories of the five-zone SMBs with different column numbers were obtained for each component at its corresponding product port. The results are compared in terms of the column number in Figure 6. It is evident that as the column number per zone increases, the product concentration profiles have less fluctuation. Ultimately, the five-zone SMB with an infinite number of columns per zone, which indeed corresponds to the case of a five-zone TMB, gives a constant concentration profile as shown in Figure 6.

The concentrations in the above effluent histories represent the instantaneous ones at cyclic steady state. For the quantitative comparison of the above effluent histories, the instantaneous concentration was averaged over a switching period for each five-zone SMB with a different column number. The resulting averaged concentrations are compared in terms of the column

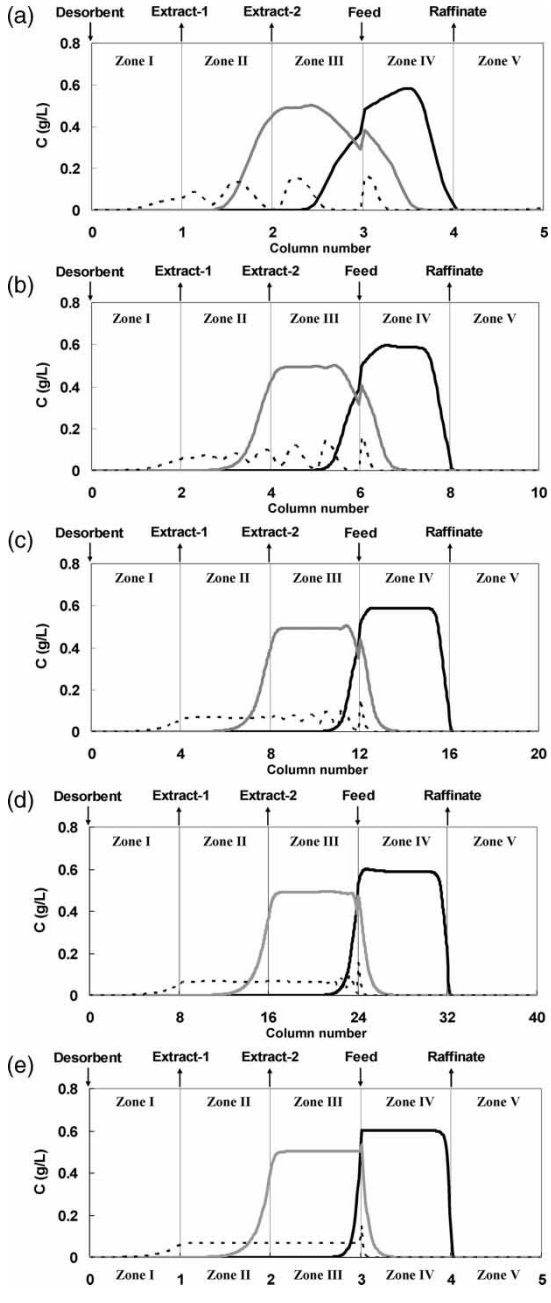


***Figure 5.*** Mid-step column profiles at cyclic steady state in the five-zone SMB with an increasing number of columns per zone. (a) 1 – 1 – 1 – 1 – 1, (b) 2 – 2 – 2 – 2 – 2, (c) 4 – 4 – 4 – 4 – 4, (d) 8 – 8 – 8 – 8 – 8, (e) ∞ – ∞ – ∞ – ∞ – ∞ (TMB). ▬: component A: ▬: component B: – – – component C.

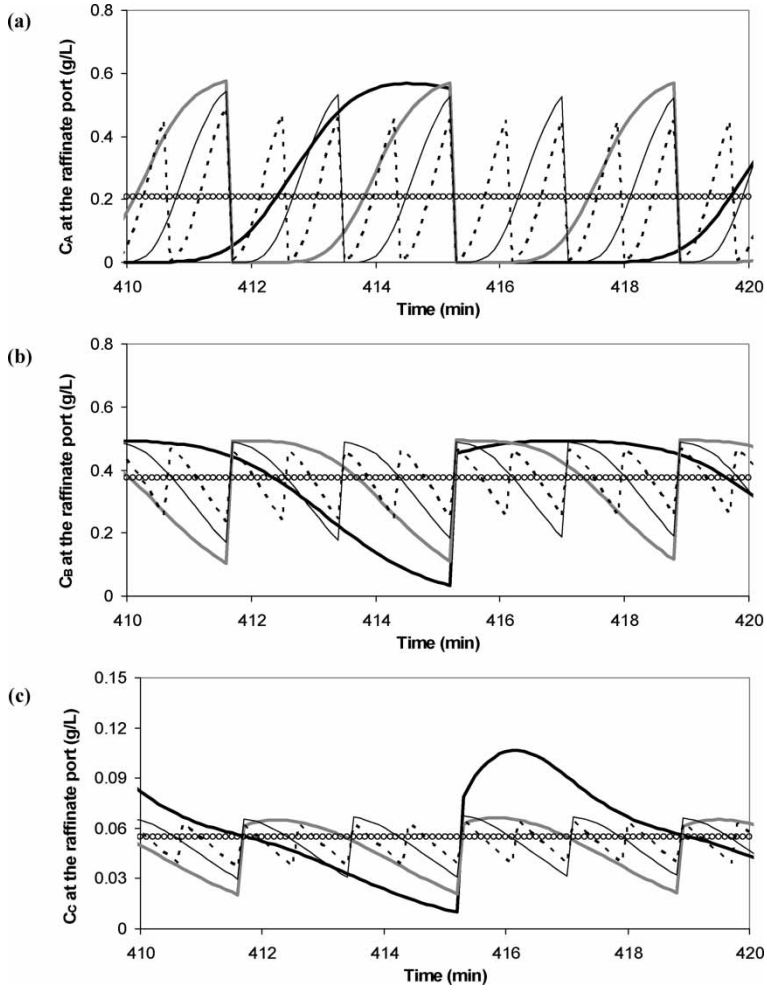


***Figure 6.*** Effluent histories at cyclic steady state in the five-zone SMB with an increasing number of columns per zone. (a) Concentration of A at the raffinate port. (b) Concentration B at the extract 2 port. (c) Concentration of C at the extract 1 port. ▬: 1 – 1 – 1 – 1 – 1, ▬: 2 – 2 – 2 – 2 – 2,: —— 4 – 4 – 4 – 4 – 4,: - - - 8 – 8 – 8 – 8 – 8, oooooo: ∞ – ∞ – ∞ – ∞ – ∞ (TMB).

number in Figure 7. Notice, that the averaged concentrations of A and B in their corresponding product streams are little affected by a change in the column number (Figure 7a). Even the concentrations of A and B from the five-zone TMB, which is equivalent to the five-zone SMB with an infinite number of columns per zone, are close to the averaged concentrations of A and B from the five-zone SMBs with a finite number of columns per zone. A similar trend can also be found in a classical four-zone SMB and TMB

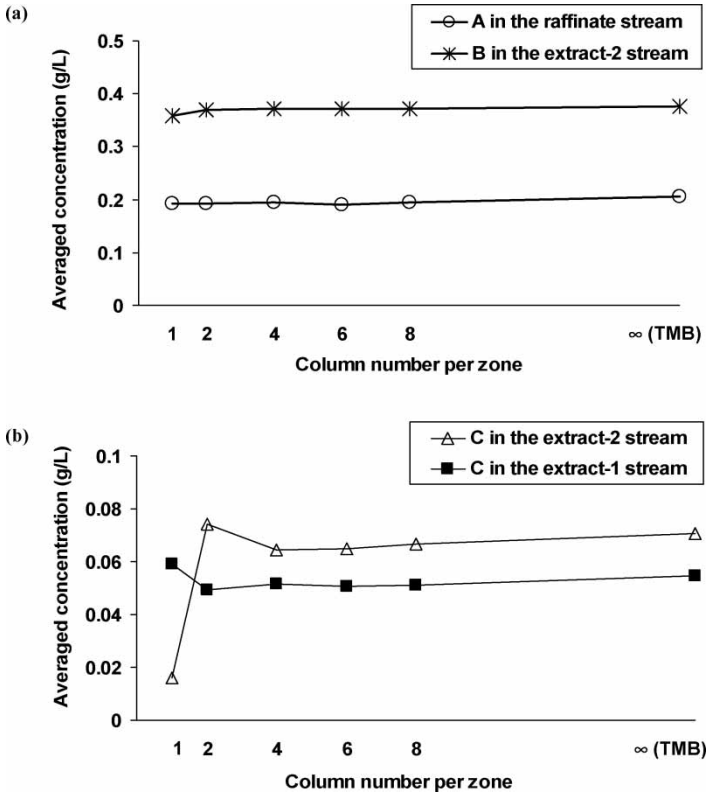


***Figure 7.*** Averaged concentration of each component at the outlet port at cyclic steady state in the five-zone SMB with an increasing number of columns per zone. (a) A in the raffinate stream and B in the extract 2 stream. (b) C in the extract 2 stream and C in the extract 1 stream.

for binary separation.[1] Such similarity may be ascribed to the fact that the zones II to V in the five-zone SMB take charge of the separation between A and B in the same manner as in a classical four-zone SMB for binary separation.

By contrast, the averaged concentrations of C in the extract 1 and the extract 2 streams exhibit a clear variation with respect to the column number, and in particular when the column number per zone is varied from one to two. As shown in Figure 7b, the averaged concentration of C in the extract 2 stream is kept low when each zone contains only one column. This condition will be favorable for the purity of B because component C corresponds to an impurity in the extract 2 stream. However, if more than two columns are allocated to each zone, the averaged concentration of C is significantly increased, resulting in severe contamination of product B with the impurity C.

The aforementioned phenomenon can be well understood using the column profiles in Figure 5. Close observation of the column profiles and the extract 2 port location reveals that the passage of component C through the extract 2 port can be effectively prevented when the solute bands of C are properly scattered in different zones, as shown in Figure 5a. At this time, the extract 2 port can be located in the region free of C between the two adjacent solute bands of C (Figure 5a), leading to high purity of B in the extract 2 stream. Such aspect of the solute band distribution, however, fades away as the column number per zone increases. As shown in Figures 5b to 5e, the solute bands of C are no longer scattered but gradually combined into a single solute band, which eventually ranges from zone I through zone IV. Under such circumstances, a considerable amount of component C must pass through the extract 2 port located between zones II and III, resulting in a significant reduction in the purity of B in the extract 2 stream. Simultaneously, a noticeable decrease in the averaged concentration of C at its corresponding product port, i.e., the extract 1 port also occurs as a result of the loss of C through the extract 2 port (Figure 7b). For these reasons, the averaged concentrations of C in the two extract streams for a five-zone SMB with one column per zone cannot be accurately predicted from its corresponding five-zone TMB model.



## Effect of Subdividing the Adsorbent Bed on the Separation Performance of the Five-Zone SMB Chromatography

In the previous sections, some noticeable differences in the wave dynamics and the effluent histories were found among the five-zone SMBs with different column numbers. Such differences will also affect the separation performance of the five-zone SMB. It is, therefore, worth discussing whether there is any notable tendency in the separation performance of the five-zone SMB with respect to the column number per zone.

The separation performance is usually evaluated by the product purities. As stated previously, the product purities of the five-zone SMB are in effect determined by the migration behaviors of adsorption and desorption waves of the three nucleoside components. To ensure high product purities, the migration range of each wave should be confined within its corresponding zone from the beginning to the end of a step at cyclic steady state. Because each wave shows a different migration behavior with respect to the column number, the product purities can also be influenced by the column number.

To check the aforementioned effect, the column profiles of the five-zone SMBs with different column numbers were obtained at the beginning and the end of a step at cyclic steady state. The results are presented in Figures 8 to 10, where the solid lines indicate the profiles at the beginning of a step and the dashed lines the profiles at the end of a step. As the column number per zone increases, the adsorption wave of B seems to be better confined within

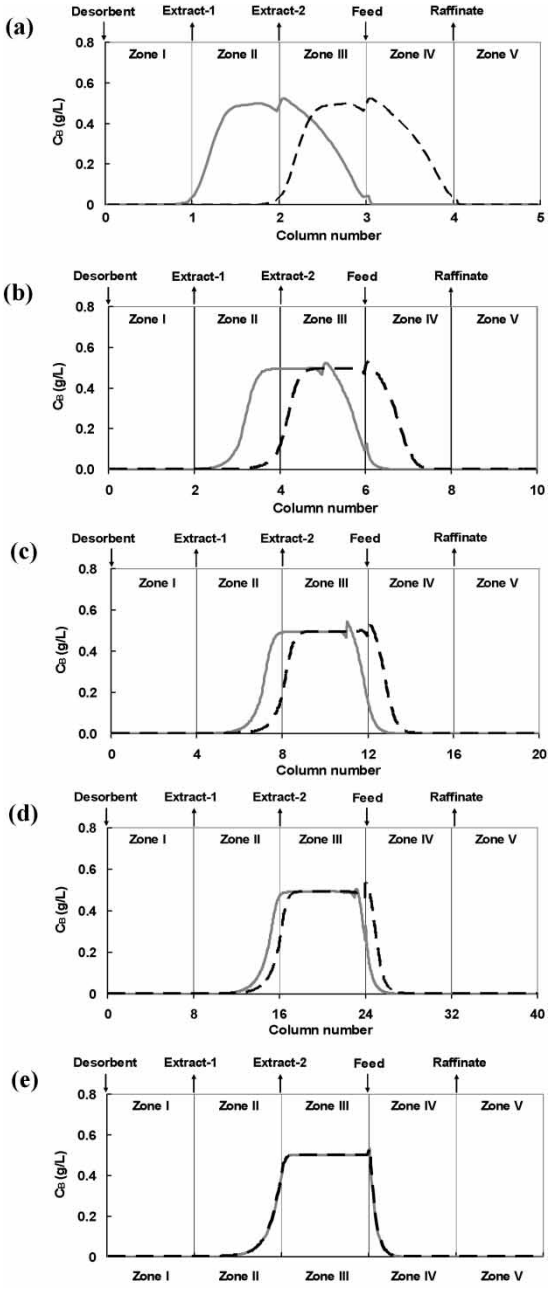


***Figure 8.*** Column profiles of component B obtained at the beginning (—) and at the end (- - -) of a step at cyclic steady state in the five-zone SMB with an increasing number of columns per zone. (a) 1 – 1 – 1 – 1 – 1, (b) 2 – 2 – 2 – 2 – 2, (c) 4 – 4 – 4 – 4 – 4. (d) 8 – 8 – 8 – 8 – 8, (e) ∞ – ∞ – ∞ – ∞ – ∞ (TMB).

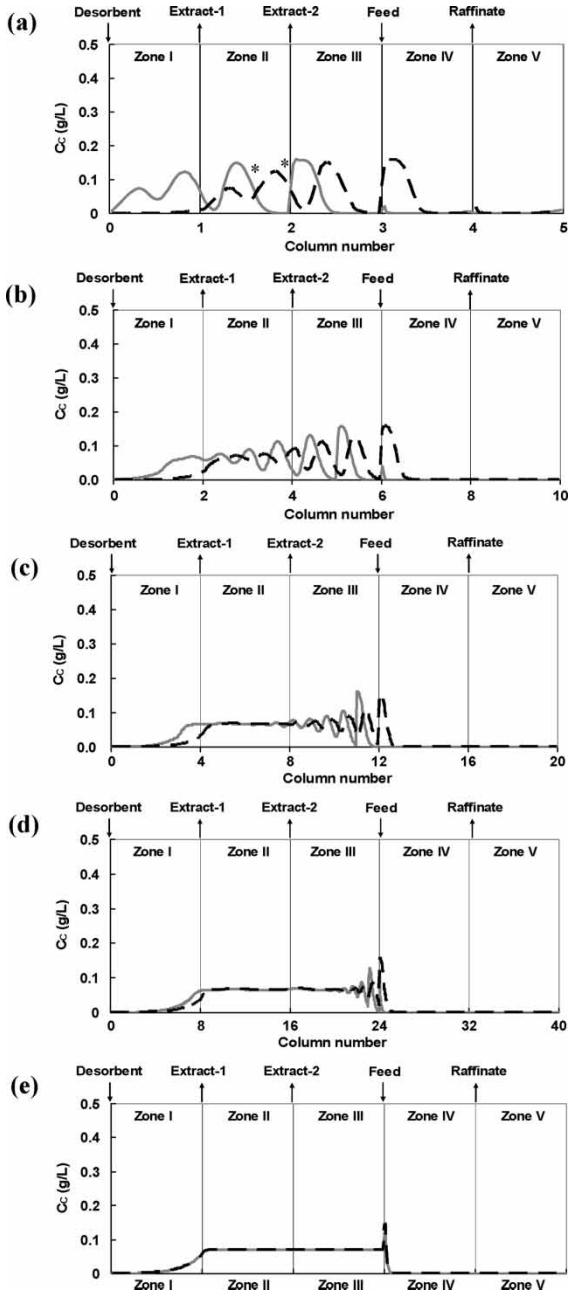


*Figure 9.* Column profiles of component C obtained at the beginning (—) and at the end (- - -) of a step at cyclic steady state in the five-zone SMB with an increasing number of columns per zone. (a) 1 – 1 – 1 – 1 – 1, (b) 2 – 2 – 2 – 2 – 2, (c) 4 – 4 – 4 – 4 – 4, (d) 8 – 8 – 8 – 8 – 8, (e) ∞ – ∞ – ∞ – ∞ – ∞ (TMB).

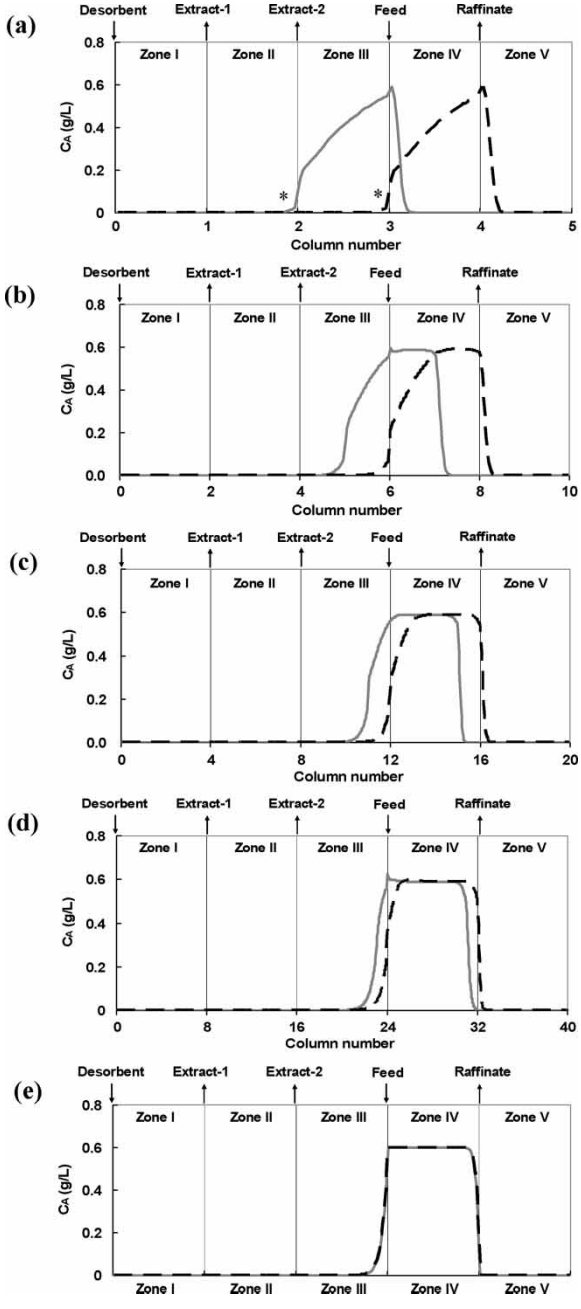


***Figure 10.*** Column profiles of component A obtained at the beginning (▬) and at the end (- - -) of a step at cyclic steady state in the five-zone SMB with an increasing number of columns per zone. (a) 1 – 1 – 1 – 1 – 1, (b) 2 – 2 – 2 – 2 – 2, (c) 4 – 4 – 4 – 4 – 4, (d) 8 – 8 – 8 – 8 – 8, (e) ∞ – ∞ – ∞ – ∞ – ∞ (TMB).

zone IV throughout the entire switching period, and its end thus becomes father away from the raffinate port (Figure 8). Also, the desorption wave of C becomes father away from the desorbent port as the column number increases (Figure 9), which can prevent the possible wrap around of component C throughout the bed. Obviously, such wave behaviors resulting from the increase of column number will be favorable for the purity of A in the raffinate stream. This tendency is well demonstrated in Figure 11, where the purity of A is plotted against the column number per zone. Note, that the five-zone SMB with one column per zone gives a purity of about 97% for the product A, whereas the five-zone SMB with more than two columns per zone leads to a purity of nearly 100%.

For similar reasons, the purity of C in the extract 1 stream is improved by placing more than two columns instead of one column in each zone (Figure 11). In this case, an increase in the column number makes the adsorption wave of A and the desorption wave of B move farther away from the extract 1 port (Figures 8 and 10), resulting in higher purity of C.

So far, only the purities of A and C have been discussed with respect to the column number per zone. The remaining one to be discussed is the purity of B in the extract 2 stream. The key waves affecting the purity of B in the extract 2 stream are the desorption wave of A in zone III and the adsorption wave of C in zone II as indicated by asterisks in Figures 9a and 10a. As the column number per zone is increased from one to two, the desorption wave of A in zone III becomes more distant from the extract 2 port (Figure 10), which is favorable for the purity of B. In contrast, the adsorption wave of C in zone II (indicated by asterisks) becomes closer to the extract 2 port and eventually passes through the extract 2 port (Figure 9), which is unfavorable for the purity of B. Since the unfavorable effect surpasses the favorable effect to a large extent, the net purity of B has a significant reduction as shown in Figure 11. In case more than four columns are placed in each zone, component C no longer

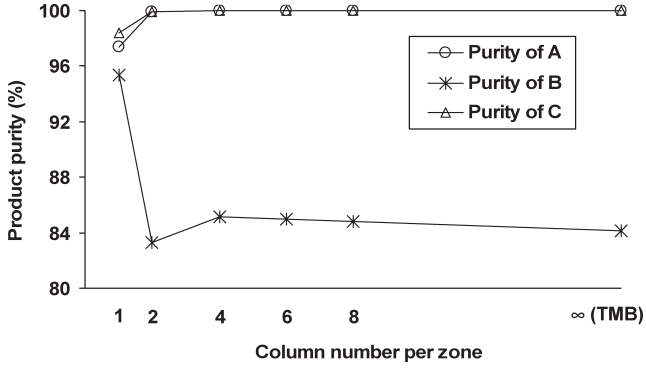


***Figure 11.*** Effect of the column number per zone on the product purities in the five-zone SMB.

maintains its adsorption wave in zone II but forms a plateau region across the extract 2 port as shown in Figures 9c to 9e. As a result, the purity of B exhibits only a slight variation with respect to the column number per zone if more than four columns are placed in each zone (Figure 11).

In summary, the purities of A and C are improved by increasing the column number per zone, and such effect is the most pronounced when the column number is increased from one to more than two. By contrast, the purity of B is significantly decreased when each zone contains more than two columns instead of one column, and such phenomenon is mostly related to a change in the wave evolution of C in accordance with an increase in the column number per zone.

## CONCLUSION



For a five-zone SMB aiming at the separation of a ternary nucleoside mixture into three different pure fractions, the effects of subdividing the adsorbent bed on the wave dynamics and separation performance were investigated. Such effects were generated by increasing the number of columns per zone while the total bed volume, zone length, and zone flow rates remained unchanged. Only the step time and single column length were reduced while the port velocity was kept constant.

The results indicate that the subdivision of the adsorbent bed has a pronounced effect on the wave dynamics of the five-zone SMB. For the lowest affinity (A) and the intermediate affinity (B) components, the plateaus of their solute bands become smoother as the number of columns per zone increases. In the extreme case where each zone contains an infinite number of columns, the plateaus of the solute bands becomes completely even, which virtually corresponds to the case of the five-zone TMB. By contrast, the average concentrations of A and B at their corresponding product ports are little affected by a change in the column number per zone, indicating that the five-zone TMB model can be exploited to estimate the average product concentrations of A and B in the five-zone SMB with a finite number of columns per zone.

In the case of the solute bands of the highest affinity component (C), they are first scattered in several zones of the five-zone SMB with one column per zone. If the column number per zone increases, the scattered solute bands of C are gradually merged, resulting in a seemingly single solute band of C with a wavy plateau. When the column number per zone approaches infinity, the wavy plateau becomes flat and the column profiles of the five-zone SMB approach those of the five-zone TMB.

Such behavior of the C solute bands gives rise to a visible change in the average concentrations of C at the two extract ports, especially when the scattered solute bands of C are on the point of merging due to an increase in the column number per zone. Because, at this time, a considerable amount of component C must pass through the extract 2 port, the average

concentration of C at the extract 2 port increases accordingly, resulting in a significant reduction in the purity of B. Simultaneously, a noticeable decrease in the average concentration of C at its corresponding product port, i.e., the extract 1 port also occurs as a result of the loss of C through the extract 2 port. For these reasons, the average concentrations of C in the two extract streams, for a five-zone SMB with one column per zone, cannot be accurately predicted from its corresponding five-zone TMB model.

Unlike the purity of B, the purities of A and C represent an increasing trend as the column number per zone increases. This is because an increase in the column number per zone plays a part in narrowing down the migration ranges of the key waves affecting the purities of A and C from the beginning to the end of a step at cyclic steady state. Such behaviors make the key waves better confined within their corresponding zones through the entire switching period, resulting in higher purity of A and C.

The results of this study are expected to serve as a useful summary of five-zone SMB behaviors and as the first step for the development of new strategies on five-zone SMB performance.



## NOMENCLATURE

| | |
|---|---|
| $C_F$ | feed concentration, g/L |
| D | desorbent flow rate, mL/min |
| $d_c$ | column diameter, cm |
| $E_1$ | extract 1 flow rate, mL/min |
| $E_2$ | extract 2 flow rate, mL/min |
| F | feed flow rate, mL/min |
| $L_c$ | single column length, cm |
| $N_{cln}$ | number of columns |
| PI | purity index, % |
| PurA | purity of A, % |
| PurB | purity of B, % |
| PurC | purity of C, % |
| $Q_j$ | flow rate in zone j, mL/min |
| R | raffinate flow rate, mL/min |
| $t_s$ | step time, min |
| *w* | weighting factor |
| $\Delta P_{unit}$ | pressure drop through an SMB unit, psi |

## ACKNOWLEDGMENTS

This work was supported by the Korea Research Foundation Grant funded by the Korean Government (MOEHRD) (KRF-2005-041-D00187). The author is grateful to Prof. Nien-Hwa Linda Wang from Purdue University.

## REFERENCES


1. Chu, K.H.; Hashim, M.A. Simulated countercurrent adsorption processes: a comparison of modeling strategies. Chem. Eng. J. **1995**, *56*, 59–65.
2. Mun, S.; Yi, X.; Wang, N.-H.L. Strategies to control batch integrity in size-exclusion simulated moving bed chromatography. Ind. Eng. Chem. Res. **2005**, *44*, 3268–3283.
3. Hidajat, K.; Ching, C.B.; Ruthuven, D.M. Simulated counter-current adsorption process: a theoretical analysis of the effect of subdividing the adsorbent bed. Chem. Eng. Sci. **1986**, *11*, 2953–2956.
4. Ma, Z.; Wang, N.-H.L. Standing wave analysis of SMB chromatography: linear systems. AIChE J. **1997**, *43*, 2488–2508.
5. Beste, Y.A.; Arlt, W. Side-stream simulated moving-bed chromatography for multicomponent separation. Chem. Eng. Technol. **2002**, *25*, 956–962.
6. Kim, J.K.; Zang, Y.; Wankat, P.C. Single-cascade simulated moving bed systems for the separation of ternary mixtures. Ind. Eng. Chem. Res. **2003**, *42*, 4849–4860.
7. Wang, X.; Ching, C.B. Chiral separation of $\beta$-blocker drug (nadolol) by five-zone simulated moving bed chromatography. Chem. Eng. Sci. **2005**, *60*, 1337–1347.
8. Hur, J.S.; Wankat, P.C. Hybrid simulated moving bed and chromatography systems for center-cut separation from quaternary mixtures: linear isotherm systems. Ind. Eng. Chem. Res. **2006**, *45*, 8713–8722.
9. Paredes, G.; Abel, S.; Babler, M.U.; Mazzotti, M.; Morbidelli, M.; Stadler, J. Analysis of a simulated moving bed operation of three fraction separations (3F-SMB). Ind. Eng. Chem. Res. **2004**, *43*, 6157–6167.
10. Kasat, R.B.; Gupta, S.K. Multi-objective optimization of an industrial fluidized-bed catalytic cracking unit (FCCU) using genetic algorithm (GA) with the jumping genes operator. Comput. Chem. Eng. **2003**, *27*, 1785–1800.
11. Zhang, Z.; Hidajat, K.; Ray, A.K.; Morbidelli, M. Multiobjective optimization of SMB and varicol process for chiral separation. AIChE J. **2002**, *48*, 2800–2816.
12. Subramani, H.J.; Hidajat, K.; Ray, A.K. Optimization of simulated moving bed and varicol processes for glucose-fructose separation. Chem. Eng. Res. Des. **2003**, *81*, 549–567.
13. Zhang, Z.; Mazzotti, M.; Morbidelli, M. Multiobjective optimization of simulated moving bed and varicol processes using a genetic algorithm. J. Chromatogr. A **2003**, *989*, 95–108.
14. Chung, S.F.; Wen, C.Y. Longitudinal dispersion of liquid flowing through fixed and fluidized beds. AIChE J. **1968**, *14*, 857–866.
15. Zang, Y.F.; Wankat, P.C. Variable flow rate operation for simulated moving bed separation systems: simulation and optimization. Ind. Eng. Chem. Res. **2003**, *42*, 4840–4848.
16. Hur, J.S.; Wankat, P.C. New design of simulated moving bed for ternary separations. Ind. Eng. Chem. Res. **2005**, *44*, 1906–1913.
17. Hur, J.S.; Wankat, P.C. Two zone SMB/chromatography for center-cut separation from ternary mixtures: linear isotherm systems. Ind. Eng. Chem. Res. **2006**, *45*, 1426–1433.
18. Ergun, S. Flow through packed columns. Chem. Eng. Prog. **1952**, *48*, 89–94.

19. Mun, S.; Wang, N.-H.L.; Koo, Y.M.; Yi, S.C. Pinched wave design of a four-zone SMB for linear adsorption systems with significant mass transfer effects. Ind. Eng. Chem. Res. **2006**, *45*, 7241–7250.

Received January 5, 2008
Accepted February 13, 2008
Manuscript 6269